



## Design of a self-unfolding delivery concept for oral administration of macromolecules

Jørgensen, Jacob R.; Thamdrup, Lasse H.E.; Kamguyan, Khorshid; Nielsen, Line H.; Nielsen, Hanne M.; Boisen, Anja; Rades, Thomas; Müllertz, Anette

*Published in:*  
Journal of controlled release

*Link to article, DOI:*  
[10.1016/j.jconrel.2020.10.024](https://doi.org/10.1016/j.jconrel.2020.10.024)

*Publication date:*  
2021

*Document Version*  
Peer reviewed version

[Link back to DTU Orbit](#)

*Citation (APA):*  
Jørgensen, J. R., Thamdrup, L. H. E., Kamguyan, K., Nielsen, L. H., Nielsen, H. M., Boisen, A., Rades, T., & Müllertz, A. (2021). Design of a self-unfolding delivery concept for oral administration of macromolecules. *Journal of controlled release*, 329, 948-954. <https://doi.org/10.1016/j.jconrel.2020.10.024>

---

### General rights

Copyright and moral rights for the publications made accessible in the public portal are retained by the authors and/or other copyright owners and it is a condition of accessing publications that users recognise and abide by the legal requirements associated with these rights.

- Users may download and print one copy of any publication from the public portal for the purpose of private study or research.
- You may not further distribute the material or use it for any profit-making activity or commercial gain
- You may freely distribute the URL identifying the publication in the public portal

If you believe that this document breaches copyright please contact us providing details, and we will remove access to the work immediately and investigate your claim.

# 1 Design of a self-unfolding delivery concept for oral administration of 2 macromolecules

3  
4 *Jacob R. Jørgensen<sup>a</sup>, Lasse H. E. Thamdrup<sup>b</sup>, Khorshid Kamguyan<sup>b</sup>, Line H. Nielsen<sup>b</sup>,  
5 Hanne M. Nielsen<sup>c</sup>, Anja Boisen<sup>b</sup>, Thomas Rades<sup>a</sup>, Anette Müllertz<sup>d,\*</sup>*

6  
7 <sup>a</sup> Department of Pharmacy, University of Copenhagen, Universitetsparken 2, 2100 Copenhagen,  
8 Denmark  
9 *E-mail addresses:* jacob.r.joergensen@sund.ku.dk, thomas.rades@sund.ku.dk

10  
11 <sup>b</sup> Center for Intelligent Drug Delivery and Sensing Using Microcontainers and Nanomechanics  
12 (IDUN), Department of Health Technology, Technical University of Denmark, Ørsteds Plads, 2800  
13 Kgs. Lyngby, Denmark  
14 *E-mail addresses:* lhth@dtu.dk, khokam@dtu.dk, lihan@dtu.dk, aboi@dtu.dk

15  
16 <sup>c</sup> Center for Biopharmaceuticals and Biobarriers in Drug Delivery, Department of Pharmacy,  
17 University of Copenhagen, Universitetsparken 2, 2100 Copenhagen, Denmark  
18 *E-mail address:* hanne.morck@sund.ku.dk

19  
20 <sup>d</sup> Bioneer:FARMA, Department of Pharmacy, University of Copenhagen, Universitetsparken 2,  
21 2100 Copenhagen, Denmark

22  
23 \* Corresponding author at: Universitetsparken 2, 2100 Copenhagen, Denmark  
24 *E-mail address:* anette.mullertz@sund.ku.dk (A. Müllertz)

25  
26 **Keywords:** Oral insulin; Delivery devices; Elastomers; Permeation enhancers; Protease inhibitors;  
27 Polydimethylsiloxane

## 28 **Abstract**

29 Delivering macromolecular drugs, e.g. peptides, to the systemic circulation by oral  
30 administration is challenging due to their degradation in the gastrointestinal tract and low  
31 transmucosal permeation. In this study, the concept of an oral delivery device utilizing an  
32 elastomeric material is presented with the potential of increasing the absorption of  
33 peptides, e.g. insulin. Absorption enhancement in the intestine is proposed as a result of  
34 self-unfolding of a polydimethylsiloxane foil upon release from enteric coated capsules. A  
35 pH-sensitive polymer coating prevents capsule disintegration until arrival in the small  
36 intestine where complete unfolding of the elastomeric foil ensures close contact with the  
37 intestinal mucosa. Foils with close-packed hexagonal compartments for optimal drug  
38 loading are produced by casting against a deep-etched silicon master. Complete unfolding  
39 of the foil upon capsule disintegration is verified *in vitro* and the insulin release profile of  
40 the final delivery device confirms insulin protection at gastric pH. *In vivo* performance is  
41 evaluated with the outcome of quantifiable plasma insulin concentrations in all rats  
42 receiving duodenal administration of the novel delivery device. By taking advantage of  
43 elastomeric material properties for drug delivery, this approach might serve as inspiration

44 for further development of commercially viable biocompatible devices for oral delivery of  
45 macromolecules.

## 46 **1. Introduction**

47 Oral administration of macromolecules, e.g. peptides and proteins, has been attempted for  
48 decades in order to improve patient compliance [1,2]. Previous initiatives have mainly  
49 focused on incorporating protease inhibitors, such as soybean trypsin inhibitor (STI), and  
50 permeation enhancers (PEs) in order to decrease enzymatic degradation while increasing  
51 absorption from the intestine [1,3]. Co-formulating peptides with such active excipients in  
52 tablets or capsules has been the strategy in several preclinical and clinical assessments  
53 [2]. However, innovative oral delivery devices have, over the last few years, challenged the  
54 conventional concepts of oral systemic absorption by proposing the application of  
55 gastrointestinal (GI) injections resulting in >10% oral bioavailability relative to  
56 subcutaneous (SC) injection [4–7]. Physical perforation of the outer layers of the  
57 absorptive barriers has thereby become an interesting alternative to excipient-induced  
58 absorption of macromolecules [8]. While both approaches are interesting platforms for  
59 peptide delivery, the risks of repeated administrations of PEs and GI-injections are  
60 unknown. Nevertheless, the constant regeneration of the epithelial cells along the GI-tract  
61 is a recurring argument for the therapeutic relevance of temporary barrier disruption  
62 regardless of being induced by PEs or by physical perforation [5,9,10].

63 The status as food additive, Generally Recognized As Safe (GRAS) or inactive ingredient  
64 held by some PEs, e.g. sodium caprate (C<sub>10</sub>), salcaprozate sodium (SNAC) and sodium  
65 dodecyl sulfate (SDS), have rendered them popular choices in industrial formulation  
66 strategies [8]. Notably, C<sub>10</sub> and SNAC have proven beneficial, and have led to the  
67 achievement of therapeutic oral bioavailability of insulin and the glucagon-like peptide-1  
68 agonist, semaglutide, respectively. Moreover, the latter formulation has received approval  
69 from the U.S. Food & Drug Administration [11,12]. Thereby, PE-based formulations have  
70 proven to be commercially viable, yet they still need to compensate with higher peptide  
71 doses due to relatively low oral bioavailability compared to the GI-injecting delivery devices  
72 [5,7,11,12]. On the other hand, while the GI-injecting devices are innovative from an  
73 engineering perspective, their complexity is likely to impede the rate of potential mass  
74 production compared to that of conventional tablets and capsules [4,5,7]. A solution to the  
75 high doses required in PE-based oral dosage forms has previously been proposed with  
76 unidirectional-releasing devices capable of creating local environments of high

77 concentrations of peptide and excipients along the intestinal absorptive barrier [13–16].  
78 Such confinement would increase the local effect of active excipients, e.g. PEs and  
79 protease inhibitors, while creating a steep peptide concentration gradient across the  
80 intestinal mucosa. The proximity between the absorptive barrier and such unidirectional-  
81 releasing devices has proven of outmost importance *in vitro* with a 50% decrease in insulin  
82 absorption for every distance increase of 130  $\mu\text{m}$  from a Caco-2 cell monolayer mimicking  
83 the intestinal absorptive barrier [16].

84 Insulin release in the gastric environment can be prevented by enteric coating, but  
85 ensuring optimal unidirectional release in close proximity to the intestinal epithelium has  
86 proven challenging to attain *in vivo* [17]. Moreover, it has proven problematic to conduct *in*  
87 *vivo* studies of enteric coated capsules in rats, due to long-term gastric retention of such  
88 dosage forms [18]. Previously, this issue has been circumvented by pre-administration of  
89 the prokinetic agent, metoclopramide, to promote gastric emptying, or by direct intestinal  
90 insertion of the dosage form through an incision in the proximal small intestine [13,14,19].  
91 Thus, such preclinical *in vivo* studies either alter the normal peristalsis by inclusion of a  
92 prokinetic agent or might even possess the risk of absorption at the site of intestinal  
93 perforation, thereby causing a false positive result.

94 An alternative approach to preclinical *in vivo* studies of enteric coated capsules in rats was  
95 used in the present work, without neither penetrating the GI-tract mucosa nor using  
96 prokinetic agents. This *in vivo* approach, which will be discussed in more detail below,  
97 contributed to the overall aim of the present study, namely to conceptualize and design an  
98 oral device capable of guaranteeing optimal unidirectional drug and excipient release in  
99 close proximity to the intestinal mucosa. The design comprises an elastomeric self-  
100 unfolding foil with cavities for drug- and excipient loading rolled up in an enteric coated  
101 gelatin capsule. The key to successfully achieving unidirectional release in close proximity  
102 to the intestinal mucosa thus lies in the elastomeric nature of the material ensuring purely  
103 elastic deformation. For the present proof-of-concept study, polydimethylsiloxane (PDMS)  
104 was chosen as the foil material due to its elastomeric properties, while the approximately 6  
105 kDa peptide hormone, insulin, was chosen as the model macromolecular drug.

## 106 2. Materials and Methods

### 107 2.1 Materials

108 Human recombinant insulin, SDS and dibutyl sebacate were acquired from Sigma-Aldrich  
109 (St. Louis, MO, USA). STI was bought from Thermo Fisher Scientific (Waltham, MA, USA)  
110 and SYLGARD™ 184 silicone elastomer kit from Dow Chemical Company (Midland, MI,  
111 USA). Eudragit® L 100 and L100-55 were both obtained from Evonik (Essen, Germany).  
112 Midazolam (5 mg mL<sup>-1</sup>) was procured from Hameln (Gloucester, UK) whereas Hypnorm  
113 (fentanyl, 0.315 mg mL<sup>-1</sup>; fluanisone 10 mg mL<sup>-1</sup>) was acquired from Skanderborg  
114 Pharmacy (Skanderborg, Denmark), and pentobarbital/Euthanimal (400 mg mL<sup>-1</sup>) from  
115 Alfasan (Woerden, Netherlands). All additional chemicals and solvents were at least of  
116 analytical grade and obtained from commercial suppliers. Ultrapure water was used  
117 throughout the studies purified by an Ultra Clear UV system (Evoqua Water Technologies,  
118 Pittsburgh, PA, USA).

### 119 2.2 Fabrication of hexagonal patterned silicon master

120 For optimal results during the deep anisotropic etch into the silicon (Si) substrate, a SiO<sub>2</sub>  
121 hard mask was used. A 1 μm thick wet thermal oxide was grown in a horizontal furnace  
122 (Tempress, Vaassen, The Netherlands) and masked using the conventional positive  
123 photoresist AZ® 5214 E (MicroChemicals, Ulm, Germany). In order to increase resist  
124 adhesion, hexamethyldisilazane was deposited as part of the procedure for spin coating the  
125 1.5 μm thick resist layer. The UV-exposure was conducted using an MLA100 Tabletop  
126 Maskless Aligner (Heidelberg Instruments, Heidelberg, Germany) and a dose of 90 mJ cm<sup>-2</sup>  
127 before developing the exposed pattern for 90 s using AZ® 726 MIF (MicroChemicals,  
128 Ulm, Germany). Subsequently, the hexagonal pattern was transferred into the oxide layer  
129 using an Advanced Oxide Etcher (STS MESC Multiplex ICP, SPTS Technologies,  
130 Newport, UK) with C<sub>4</sub>F<sub>8</sub> and H<sub>2</sub> as the reactive gasses. The remaining resist mask was  
131 stripped using a combination of energetic oxygen plasma in a barrel asher (300 Semi Auto  
132 Plasma Processor, PVA TePla, Wetzlar, Germany) and submersion into concentrated  
133 H<sub>2</sub>SO<sub>4</sub> with (NH<sub>4</sub>)<sub>2</sub>S<sub>2</sub>O<sub>8</sub> salt at 80 °C. The honeycomb trenches were then etched into the  
134 Si using an inductively coupled plasma deep reactive ion etching tool (STS Pegasus,  
135 SPTS Technologies, Newport, UK). The tool utilizes a Bosch-type process for performing  
136 deep anisotropic etching of Si by alternating between Si etching using SF<sub>6</sub> and O<sub>2</sub> and  
137 sidewall passivation obtained by deposition of C<sub>4</sub>F<sub>8</sub>. The substrate temperature was kept

138 at 0 °C throughout the etching process and the substrate was cleaned using oxygen  
139 plasma and a mixture of concentrated H<sub>2</sub>SO<sub>4</sub> and H<sub>2</sub>O<sub>2</sub> (4:1 v/v, commonly referred to as  
140 piranha) before stripping the remaining oxide mask in aqueous buffered hydrofluoric acid  
141 (12%, v/v) with NH<sub>4</sub>F. As the Si master was intended for foil fabrication by means of  
142 casting with PDMS, an anti-stick coating was deposited by molecular vapor deposition  
143 (MVD 100 Molecular Vapor Deposition System, Applied Microstructures, Orbotech, Yavne,  
144 Israel). This effectively created a monolayer of 1H,1H,2H,2H-perflourodecyltrichlorosilane,  
145 which decreased the surface energy of the Si master. This in turn promoted demolding of  
146 the delicate honeycomb protrusions after the PDMS casting and ensured that elastomer  
147 rip-off was prevented, thereby preserving the pristine master for multiple replication cycles.  
148 The width and depth of the hexagonal trenches were measured by vertical scanning  
149 interferometry using a P Lu Neox 3D Optical Profiler (Sensofar Metrology, Terrassa,  
150 Spain).

### 151 *2.3 Fabrication of PDMS foil*

152 The self-unfolding elastomer foils were fabricated by casting with SYLGARD™ 184, which  
153 is a two-component product consisting of a PDMS base and a curing agent. The base  
154 resin and curing agent were mixed in a 10:1 ratio (w/w) and degassed in a desiccator for  
155 30 min prior to use. The mixture was then poured onto the silicon master and degassed in  
156 a desiccator once more in order to remove potential air bubbles, which would otherwise  
157 compromise the structure replication fidelity. The uncured PDMS replica was then kept in  
158 an oven at 37 °C overnight and the cured elastomer foil was subsequently peeled from the  
159 Si master. The topography of the foils was characterized using vertical scanning  
160 interferometry on a P Lu Neox 3D Optical Profiler (Sensofar Metrology, Terrassa, Spain). *In*  
161 *vitro* assessment of the self-unfolding properties of the foil was assessed by recording the  
162 unfolding of a PDMS foil (7 × 7 mm<sup>2</sup>) as a result of capsule disintegration in water at 37 °C  
163 using a Dino-Lite Premier AM7013MZT digital microscope (AnMo Electronics Corporation,  
164 New Taipei City, Taiwan).

### 165 *2.4 Preparation of the final oral delivery device*

166 PDMS foils were loaded with a powder mixture of insulin, SDS as PE and STI (5:3:2,  
167 w/w/w) by tapping the powder on top of the foil and gently scraping off any excess amount.  
168 A solution of Eudragit® L 100 (1%, w/v) and dibutyl sebacate (0.1%, w/v) in isopropanol  
169 (IPA) was then spray coated on top of the hexagonal openings to seal the powder inside

170 thus enabling subsequent handling of the foils. An ExactaCoat Ultrasonic Spray System  
171 (Sono-Tek, Milton, NY, USA) was used for this purpose with an infuse rate of 0.05 mL min<sup>-1</sup>,  
172 <sup>1</sup>, path speed of 5 mm s<sup>-1</sup> and shaping air pressure of 0.02 mbar. The generator power  
173 was set to 2.2 W and an AccuMist nozzle was applied with a sample-to-nozzle distance of  
174 50 mm. Immediately after spray coating, the foils were gently rolled between the finger tips  
175 and inserted into size 9 gelatin capsules (Torpac, Fairfield, NJ, USA). A flat Si-chip was  
176 additionally coated to determine the coating thickness of Eudragit<sup>®</sup> L 100 by scanning  
177 electron microscopy using a Hitachi TM3030 Plus tabletop microscope (Hitachi High-  
178 Technologies Europe, Krefeld, Germany) with an accelerating voltage of 15 kV. Nine  
179 delivery devices were prepared in total out of which three were used for testing for the  
180 uniformity of insulin content, three were used for *in vitro* insulin release studies and three  
181 prepared for *in vivo* insulin absorption studies. The gelatin capsules for *in vivo* studies  
182 were additionally loaded with a cylindrical power magnet with a diameter and height of 2 ×  
183 1 mm, respectively (Magnetz og Magnordic, Hvidovre, Denmark). Enteric coating of the  
184 gelatin capsules was carried out by two dip coating cycles, first dipping the capsule body  
185 and afterwards the cap in Eudragit<sup>®</sup> L 100-55 (15%, w/v) and dibutyl sebacate (0.75%,  
186 w/v) in IPA giving the final delivery device. Images of the delivery device were captured  
187 with a Dino-Lite Premier AM7013MZT digital microscope (AnMo Electronics Corporation,  
188 New Taipei City, Taiwan).

## 189 *2.5 In vitro release of insulin*

190 A test for uniformity of insulin content was initially carried out by fully dissolving the content  
191 of three delivery devices in 10 mL of 50 mM phosphate buffer at pH 7 followed by reversed  
192 phase high-performance liquid chromatography (HPLC) as described below. *In vitro*  
193 release studies were carried out on a 400-DS Apparatus 7 (Agilent Technologies, Santa  
194 Clara, CA, USA) equipped with 5 mL sample cells and supplied with a 50 mM citrate buffer  
195 at pH 4 and a 50 mM phosphate buffer at pH 7. The oral delivery device was placed in 50-  
196 mesh basket sample holder and dissolution carried out under sink conditions at 37 °C for 1  
197 hour at pH 4 followed by 5 hours at pH 7 with a dip speed of 15 dips per minute. Automatic  
198 sampling of 0.5 mL was timed at 10, 30, 60, 70, 80, 90, 105, 120, 150, 180, 240 and 360  
199 min, each replaced with fresh dissolution medium. After sampling at 60 min, the total  
200 volume of citrate buffer in the sample cell was fully replaced with phosphate buffer. Insulin  
201 quantification was immediately carried out by HPLC on a Dionex Ultimate 3000 system  
202 (Thermo Fisher Scientific, Waltham, MA, USA) equipped with a Kinetex XB-C18 column  
203 (100 × 4.6 mm, 5 μm, 100 Å; Phenomenex, Torrance, CA, USA). The following gradient of

204 mobile phase A: 0.1% (v/v) trifluoroacetic acid (TFA) in water and B: 0.1% (v/v) TFA in  
205 acetonitrile was applied with a flow rate of 0.5 mL min<sup>-1</sup>: 0 – 6.0 min A:B (77:23 to 50:50,  
206 v/v), 6.0 – 6.5 min A:B (50:50 to 77:23, v/v) and 6.5 – 8.0 min A:B (77:23, v/v). Insulin was  
207 quantified as the area under the curve of the UV-absorbance peak at 276 nm against a  
208 standard curve from 10 - 1000 µg mL<sup>-1</sup> with an injection volume of 20 µL and column  
209 temperature of 22 °C.

## 210 2.6 *In vivo* absorption of insulin

211 The animal experiments were carried out in accordance with the Danish law on animal  
212 experiments as approved by the Danish Animal Experiments Inspectorate in concordance  
213 with the EU directive 2010/63/EU under license no. 2016-15-0201-00892. In total, 11 male  
214 Sprague Dawley rats (Janvier Labs, Le Genest-Saint-Isle, France) weighing 255 – 310 g  
215 were divided into three groups and housed with reversed day/night rhythm (12/12 h). The  
216 rats were fasted with *ad libitum* access to water for 12 - 14 h before initiating the study.  
217 Bolus anesthesia of fentanyl (236 µg kg<sup>-1</sup>), fluanisone (7.5 mg kg<sup>-1</sup>) and midazolam (3.75  
218 mg kg<sup>-1</sup>) was given as SC injections with repeated SC injections every 30 min of 1/3 of the  
219 bolus dose together with 0.4 mL saline. The abdominal cavity was opened to expose the  
220 gastrointestinal tract prior to dosing of all 11 rats. Two groups, each of three rats, were  
221 administered SC injections of insulin (1 IU kg<sup>-1</sup>) or saline as positive and negative control,  
222 respectively. Five rats were administered the novel delivery device directly to the stomach  
223 by the use of an oral gavage dosing tube. Gastric emptying was then facilitated by  
224 dragging the delivery device into the duodenum about 3 cm from the pylorus with an  
225 external magnet (t = 0 min). Blood samples of 200 µL were taken from the tail vein into  
226 Microvette<sup>®</sup> 200 K3E tubes (Sarstedt, Nümbrecht, Germany) at 10, 20, 30, 45, 60, 90, 120  
227 and 180 min followed by isolation of the plasma by centrifugation at 9,300 × g at 4 °C  
228 using a Microcentrifuge 5415 R (Eppendorf, Hamburg, Germany). Plasma samples were  
229 stored at -20 °C until insulin quantification was carried out by an enzyme-linked  
230 immunosorbent assay (ELISA) as described by the manufacturer (Merckodia, Uppsala,  
231 Sweden). The rats were euthanized by intracardiac injections of pentobarbital (100 mg kg<sup>-1</sup>)  
232 after the final blood sampling. Additionally, diluted *in vitro* release samples were  
233 analyzed by ELISA in order to confirm preservation of the antibody-binding moieties of  
234 insulin upon release from the prepared delivery device.

## 235 2.7 Data treatment

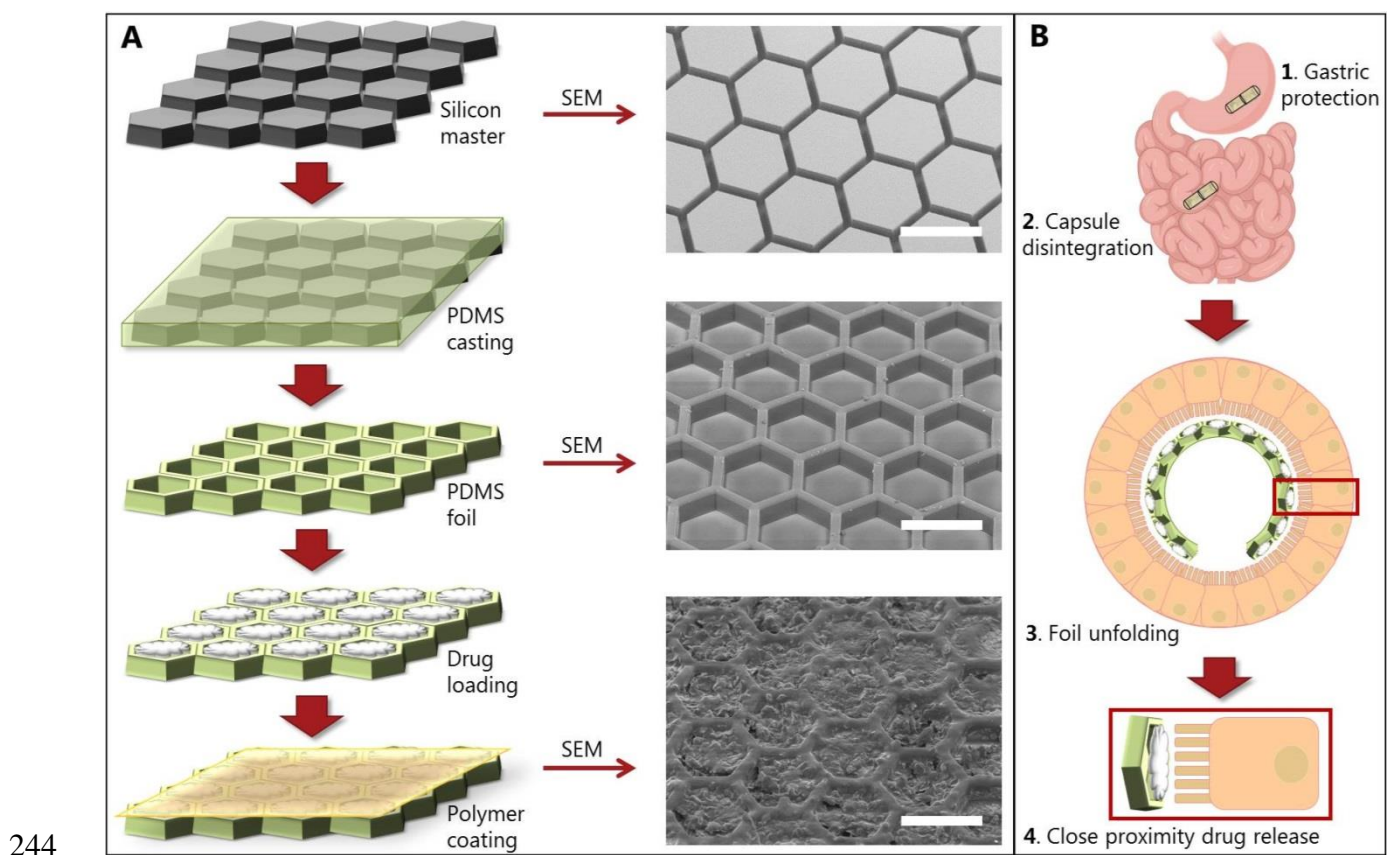


236 All data were treated using Microsoft Excel 2010 (Redmond, WA, USA) and GraphPad  
237 Prism version 8.3.0 (San Diego, CA, USA) and expressed as mean  $\pm$  standard deviation  
238 (SD) unless stated otherwise.

### 239 3. Results and discussion

#### 240 3.1 Preparation and *in vitro* assessment of the foil-based delivery device

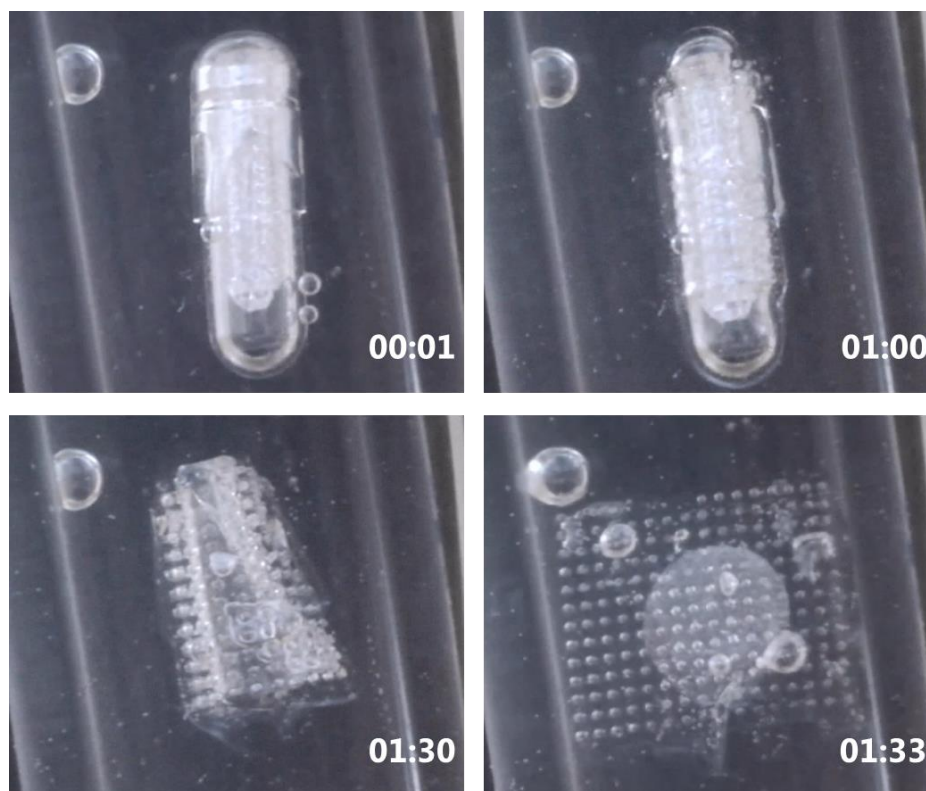
241 An overview of the preparation steps of the drug loaded elastomeric foil is shown in Fig.  
242 1A, and the principle of its proposed absorption enhancing mechanism illustrated in Fig.  
243 1B.



245 Fig. 1. Illustrations of the preparation steps and the principle of the delivery device (A) Fabrication  
246 and preparation steps of drug-loaded polydimethylsiloxane (PDMS) foil with scanning electron  
247 microscopy (SEM) images, scale bars: 400  $\mu$ m (B) Principle of the oral delivery device: Intestinal  
248 capsule disintegration is followed by foil unfolding and unidirectional drug release in close proximity  
249 to the absorptive barrier (the gastrointestinal tract schematic was created with Biorender.com) - (2-  
250 column fitting image).

251 An early 1<sup>st</sup> generation design of the cavities for drug- and excipient loading in the PDMS  
252 foil was based on previously published cylindrical devices [20,21]. This 1<sup>st</sup> generation foil

253 designed with cylindrical cavities was used for initial *in vitro* assessment of the self-  
254 unfolding properties of the PDMS foil (Fig. 2, Video S1).

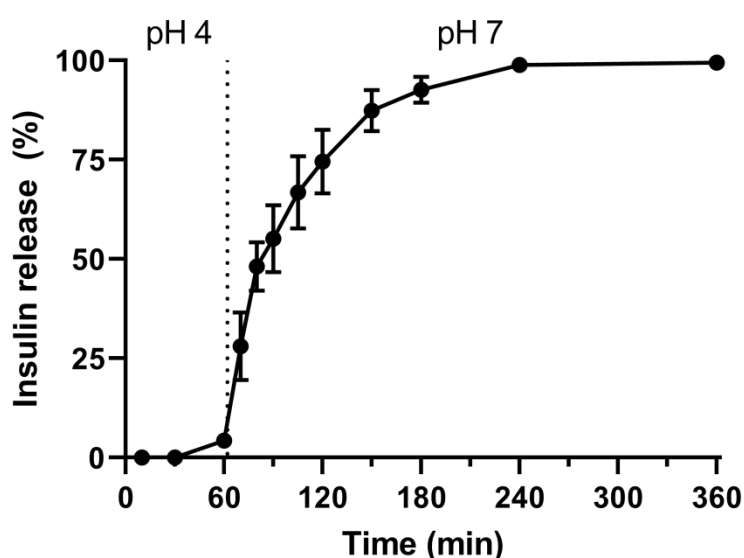


255

256 Fig. 2. Real-time disintegration of a size 9 gelatin capsule in water at 37 °C following unfolding of a  
257 PDMS foil with cylindrical cavities, timer shown as MM:SS - (1.5-column fitting image).

258 The confined shape of the foil in the gelatin capsule proved completely reversible with the  
259 foil fully restoring its original flat shape upon capsule disintegration. Inside the tubular  
260 confinement of the rat duodenum, measuring about 2.5 – 3 mm in diameter, such  
261 unfolding would thus result in close proximity between the drug loaded cavities of the foil  
262 and the intestinal mucosa [22]. To further enhance the chances of oral insulin absorption,  
263 the Si master with a close-packed hexagonal tiling was deep-etched and used for  
264 fabrication of the 2<sup>nd</sup> generation foil (Fig. 1A). The width and depth of the hexagonal  
265 trenches of the Si master were  $46 \pm 2.2$  and  $127 \pm 0.8$   $\mu\text{m}$  (mean  $\pm$  SD),  $n = 5$ ,  
266 respectively (Fig. S1A). Subsequent PDMS casting resulted in thin foils with a well-  
267 defined surface topography composed of protrusions arranged in a honeycomb pattern  
268 with an average height of  $125 \pm 0.6$   $\mu\text{m}$  (mean  $\pm$  SD,  $n = 5$ ), (Fig. S1B). The hexagonal  
269 design of the 2<sup>nd</sup> generation foil resulted in a functional area for drug- and excipient loading  
270 of 78% compared to only 21% for the 1<sup>st</sup> generation foil with cylindrical cavities. The  
271 elastomeric PDMS foil with hexagonal cavities was cut into pieces of  $7 \times 7$   $\text{mm}^2$ , and  
272 loaded with a powder mixture consisting of insulin, SDS and STI. A covering layer of

273 Eudragit<sup>®</sup> L 100, soluble in intestinal fluids with pH > 6, was applied by spray coating to  
274 seal the powder mixture inside the cavities. The covering layer, measuring approximately  
275 19  $\mu\text{m}$  (Fig. S2), thus ensured that no loss of loaded powder occurred when rolling up and  
276 inserting the foil into size 9 gelatin capsules. Finally, dip coating of the gelatin capsules  
277 was performed using Eudragit<sup>®</sup> L 100-55 to allow for rapid capsule disintegration when  
278 reaching a pH value above 5.5 in the rat small intestine. The uniformity of insulin content in  
279 the delivery devices was quantified as  $606 \pm 65 \mu\text{g}$  corresponding to  $17.5 \pm 1.9$   
280 international units (IU), when loading a powder mixture of insulin, SDS and STI (5:3:2  
281 w/w/w). Insulin release from the final delivery device was investigated *in vitro* in media  
282 simulating the pH in rat gastric and small intestinal environments to confirm sufficient  
283 capsule coating (Fig. 3). The insulin profile confirmed protection even at a relatively high  
284 gastric pH of 4, while the exchange of medium to pH 7 initiated the release of insulin,  
285 which lasted about 2 – 3 h.



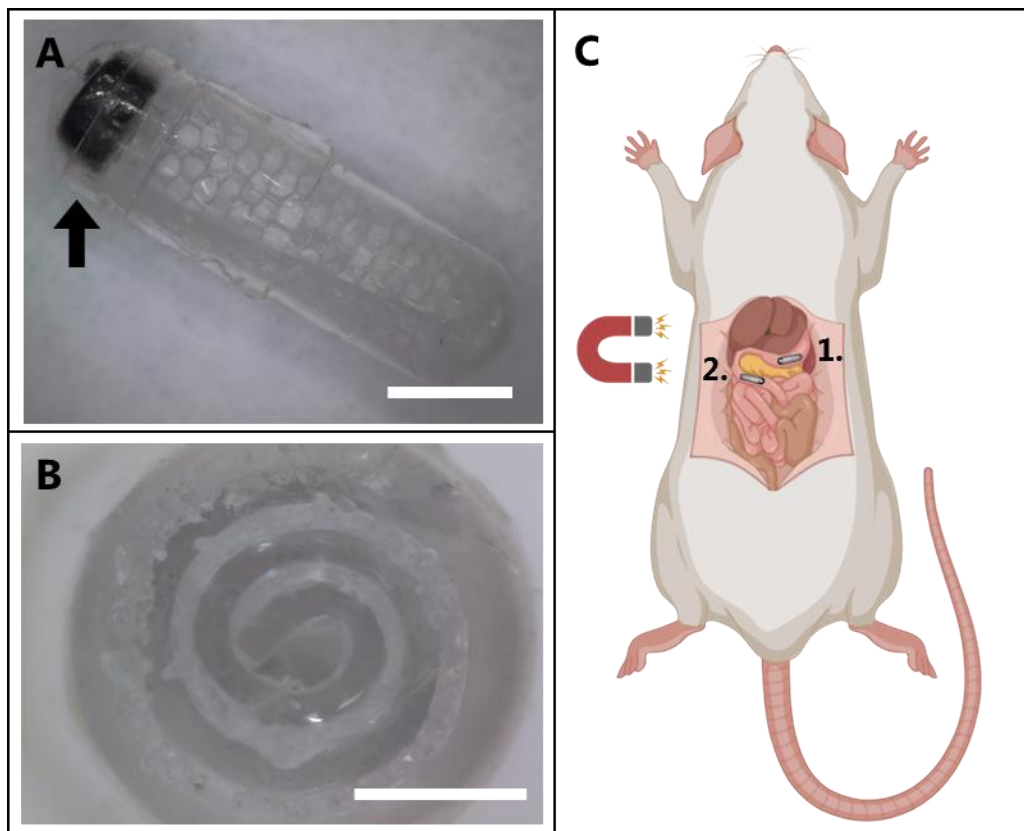
286

287 Fig. 3. *In vitro* release of insulin from the final delivery device at pH 4 followed by pH 7 under sink  
288 conditions, mean  $\pm$  standard deviation ( $n = 3$ ) - (1-column fitting image).

### 289 3.2 *In vivo* assessment

290 None of the preparation steps towards the final oral delivery device included processes  
291 that were likely to compromise the physical stability of insulin, e.g. heat, physical stress,  
292 solvents. This was supported by ELISA of diluted *in vitro* release samples, which  
293 confirmed the preservation of the antibody-binding moieties of insulin upon release from  
294 the dosage form. An alternative protocol to standard oral gavage was designed for *in vivo*  
295 evaluation of the delivery device, as studies have shown that enteric coated size 9

296 capsules may not exit the stomach upon oral administration to rats [18]. The procedure  
297 was rendered possible by including a cylindrical magnet in the capsule together with the  
298 prepared folded foil (Fig. 4A-B).

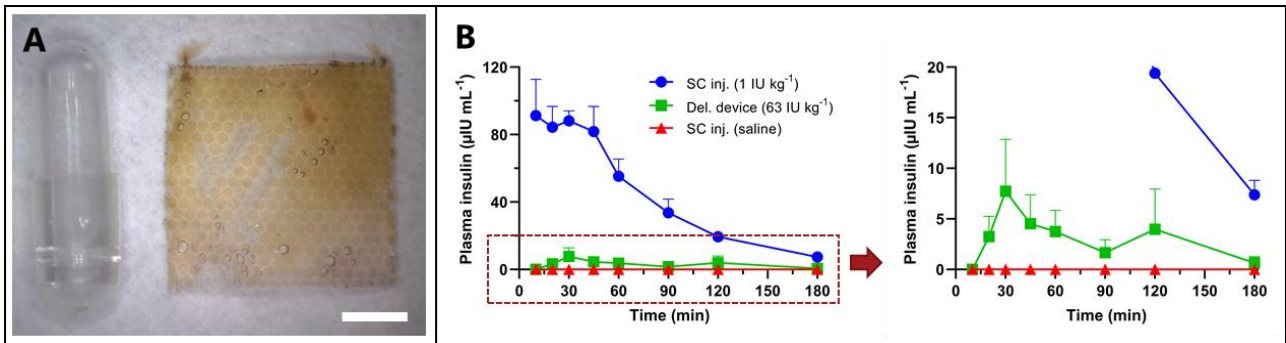


299

300 Fig. 4. *In vivo* setup for assessment of the delivery device prototype (A) The delivery device  
301 comprised of a Eudragit<sup>®</sup> L 100-55 coated size 9 gelatin capsule loaded with a magnet (arrow) and  
302 a Eudragit<sup>®</sup> L 100 coated PDMS foil loaded with insulin, sodium dodecyl sulfate and soybean  
303 trypsin inhibitor, scale bar: 2 mm (B) Cross-sectional view of the capsule showing the coiled PDMS  
304 foil inside the enteric coated size 9 gelatin capsule, scale bar: 1 mm (C) Illustration of the *in vivo*  
305 setup in two steps: 1. oral gavage of the delivery device to the stomach, 2. gastric emptying of the  
306 delivery device by the use of an external magnet (schematic created with Biorender.com) - (1.5-  
307 column fitting image).

308 The delivery device was administered by oral gavage to the stomach of anaesthetized rats  
309 followed by duodenal positioning, approximately 3 cm from the stomach, which was  
310 enabled by external magnetic maneuvering of the delivery device through the pylorus (Fig.  
311 4C). Blood samples were taken over 3 h after which fully unfolded empty PDMS foils were  
312 retrieved from the small intestines (20 – 30 cm from pylorus) with no residual remains of  
313 the gelatin capsules (Fig. 5A). Changes in blood glucose levels were not used for  
314 evaluating insulin absorption, as previous data have shown significant blood glucose

315 lowering effects by anesthesia [23]. Instead, insulin absorption was assessed by plasma  
 316 human insulin quantification by ELISA, as shown in Fig. 5B.



317  
 318 Fig. 5. *In vivo* performance of the delivery device prototype (A) PDMS foil retrieved after the *in vivo*  
 319 study and placed next to a size 9 gelatin capsule for comparison, scale bar: 2 mm (B) Plasma  
 320 insulin concentrations in rats as micro international units (IU) per mL after duodenal insertion of the  
 321 oral delivery (Del.) device compared to subcutaneous injections (SC inj.) of either insulin or saline  
 322 shown as mean + standard error of the mean ( $n = 3-5$ ) - (2-column fitting image).

323 Insulin was present in quantifiable concentrations in the plasma of all five rats receiving the  
 324 foil-based delivery device, although in relatively low concentrations compared to the SC  
 325 insulin injections. Additionally, no traces of insulin were detected in any of the negative  
 326 control plasma samples from rats receiving SC saline injections. The relative oral  
 327 bioavailability ( $F_{Rel}$ ) of the delivery device compared to the SC insulin injection was found  
 328 to be  $0.12 \pm 0.07\%$  (mean  $\pm$  standard error) based on the respective doses and the area  
 329 under the curve (AUC) of the plasma insulin profiles, calculated by the following formula.

$$330 \quad F_{Rel} = 100 \cdot \frac{AUC_{oral\ administration} \cdot 1\ IU\ kg^{-1}}{AUC_{SC\ injection} \cdot 63\ IU\ kg^{-1}}$$

331 Although the relative bioavailability achieved might appear low, oral formulations of the  
 332 antidiuretic hormone, desmopressin, have previously shown to be both therapeutically and  
 333 commercially viable with a mean relative bioavailability of 0.1% compared to SC injection  
 334 [24]. Moreover, commonly investigated peptides for oral delivery, e.g. desmopressin,  
 335 octreotide and leuprolide, might comprise a smaller absorption challenge compared to  
 336 insulin due to its larger size (51 amino acids), two-chain structure and higher susceptibility  
 337 to proteolysis [1,12,25]. However, whether higher bioavailability of such simpler peptides  
 338 could be achieved by the delivery device remains uncertain at this stage. Other oral  
 339 delivery strategies have previously resulted in a markedly higher oral insulin bioavailability  
 340 of >10%, with the highest numbers being based on physical perforation of the mucosa by



341 GI-injecting delivery devices [4-7]. Another study based on local release of thiolated  
342 polycarbophil as PE together with insulin from mucoadhesive patches has previously  
343 shown a relative oral bioavailability of 2.2% [26], suggesting that greater absorption by the  
344 present unfolding foil might be achievable by incorporating alternative PEs or by  
345 improvement of the design of the device itself. The present oral delivery principle could  
346 therefore be of general interest to both material scientists and also researchers in the field  
347 of oral delivery of peptides and even some small molecule drugs with low oral  
348 bioavailability. Class III drug compounds in the Biopharmaceutics Classification System  
349 are defined as having high solubility, but low permeability and could possibly benefit from  
350 the delivery principle of the foils by creating a local environment of high drug concentration  
351 and thus a steep gradient across the intestinal absorptive barrier [27]. However, since the  
352 current results are based on an early prototype of utilizing self-unfolding foils, further in-  
353 depth studies are needed to investigate the true potential of the delivery concept.  
354 Moreover, while the elastomer, PDMS, proved advantageous for achieving self-unfolding  
355 properties of the foil, the material possesses the notable disadvantage of not being  
356 biodegradable. While PDMS is already used for medical prosthetics and plastic surgery  
357 and generally considered nontoxic [28], its lack of disintegration represents a possible risk  
358 of accumulation in the GI-tract upon repeated oral administration. Hence biodegradability  
359 would be a considerable advantage for proceeding further from preclinical studies, yet a  
360 challenge lies in the creation of a biodegradable elastomeric foil with similar properties.  
361 Several approaches towards such materials have previously been investigated for  
362 biomedical applications based on alginate, poly(glycerol-sebacate) and even combinations  
363 of PDMS and starch [28–31]. For the purpose of oral peptide delivery, it might furthermore  
364 be of specific interest to investigate different cavity structures for drug loading and the  
365 unfolding forces of different elastomers. The interplay between those aspects might aid  
366 perforation through the intestinal mucus thus further decreasing the distance between the  
367 point of peptide- and excipient release and the absorptive barrier.

#### 368 **4. Conclusion**

369 A new oral delivery concept comprising an elastomeric PDMS foil in an enteric coated  
370 gelatin capsule was designed and tested both *in vitro* and *in vivo*. The *in vitro* studies  
371 confirmed protection at gastric pH and fully unfolding properties of the PDMS foil upon  
372 capsule disintegration. A new *in vivo* assessment for enteric coated capsules was applied  
373 to ensure gastric emptying of the designed delivery device, which showed promising  
374 properties for oral delivery of macromolecules as all rats had quantifiable insulin plasma

375 concentrations despite insulin being one of the more challenging peptides to deliver orally.  
376 In general, drug compounds with low oral bioavailability, due to low permeation and/or  
377 stability, could benefit from confinement in and subsequent release from the foil [27,32].  
378 Excipient-driven absorption mechanisms of macromolecules might furthermore gain  
379 increased efficiency from co-localization, leading to a reduced requirement of drug. Thus,  
380 the concept might have the potential to serve as a platform for a range of drug  
381 compounds, yet further studies is needed to fully unravel its potential.

## 382 **Acknowledgements**

383 This work was supported by the Danish National Research Foundation (DNRF122) and  
384 Villum Foundation (Grant No. 9301), Center for intelligent drug delivery and sensing using  
385 microcontainers and nanomechanics (IDUN) and performed in part at DTU Nanolab, the  
386 National Centre for Nano Fabrication and Characterization at the Technical University of  
387 Denmark. The graphical abstract was created with Biorender.com.

## 388 **Declaration of interest**

389 JRJ, LHET, AB, TR and AM have filed a patent application to the European Patent Office  
390 on the design of the delivery device.

## 391 **References**

- 392 [1] E. Moroz, S. Matoori, J.-C. Leroux, Oral delivery of macromolecular drugs: Where we  
393 are after almost 100 years of attempts, *Adv. Drug Deliv. Rev.* 101 (2016) 108–121.  
394 <https://doi.org/10.1016/j.addr.2016.01.010>.
- 395 [2] S. Maher, B. Ryan, A. Duffy, D.J. Brayden, Formulation strategies to improve oral  
396 peptide delivery, *Pharm. Pat. Anal.* 3 (2014) 313–336.  
397 <https://doi.org/10.4155/ppa.14.15>.
- 398 [3] A.N. Zelikin, C. Ehrhardt, A.M. Healy, Materials and methods for delivery of biological  
399 drugs, *Nat. Chem.* 8 (2016) 997–1007. <https://doi.org/10.1038/nchem.2629>.
- 400 [4] A. Abramson, E. Caffarel-Salvador, M. Khang, D. Dellal, D. Silverstein, Y. Gao, M.R.  
401 Frederiksen, A. Vegge, F. Hubálek, J.J. Water, A.V. Friderichsen, J. Fels, R.K. Kirk, C.  
402 Cleveland, J. Collins, S. Tamang, A. Hayward, T. Landh, S.T. Buckley, N. Roxhed, U.  
403 Rahbek, R. Langer, G. Traverso, An ingestible self-orienting system for oral delivery of  
404 macromolecules, *Science*. 363 (2019) 611–615.  
405 <https://doi.org/10.1126/science.aau2277>.
- 406 [5] A. Abramson, E. Caffarel-Salvador, V. Soares, D. Minahan, R.Y. Tian, X. Lu, D. Dellal,  
407 Y. Gao, S. Kim, J. Wainer, J. Collins, S. Tamang, A. Hayward, T. Yoshitake, H.-C. Lee,  
408 J. Fujimoto, J. Fels, M.R. Frederiksen, U. Rahbek, N. Roxhed, R. Langer, G. Traverso,

- 409 A luminal unfolding microneedle injector for oral delivery of macromolecules, *Nat. Med.*  
410 25 (2019) 1512–1518. <https://doi.org/10.1038/s41591-019-0598-9>.
- 411 [6] G. Traverso, C.M. Schoellhammer, A. Schroeder, R. Maa, G.Y. Lauwers, B.E. Polat,  
412 D.G. Anderson, D. Blankschtein, R. Langer, Microneedles for drug delivery via the  
413 gastrointestinal tract, *J. Pharm. Sci.* 104 (2015) 362–367.  
414 <https://doi.org/10.1002/jps.24182>.
- 415 [7] M. Hashim, R. Korupolu, B. Syed, K. Horlen, S. Beraki, P. Karamchedu, A.K. Dhalla,  
416 R. Ruffy, M. Imran, Jejunal wall delivery of insulin via an ingestible capsule in  
417 anesthetized swine—A pharmacokinetic and pharmacodynamic study, *Pharmacol.*  
418 *Res. Perspect.* 7 (2019) e00522. <https://doi.org/10.1002/prp2.522>.
- 419 [8] S. Maher, D.J. Brayden, L. Casettari, L. Illum, Application of Permeation Enhancers in  
420 Oral Delivery of Macromolecules: An Update, *Pharmaceutics.* 11 (2019) 41.  
421 <https://doi.org/10.3390/pharmaceutics11010041>.
- 422 [9] F. McCartney, J.P. Gleeson, D.J. Brayden, Safety concerns over the use of intestinal  
423 permeation enhancers: A mini-review, *Tissue Barriers.* 4 (2016) e1176822.  
424 <https://doi.org/10.1080/21688370.2016.1176822>.
- 425 [10] N. Barker, Adult intestinal stem cells: critical drivers of epithelial homeostasis and  
426 regeneration, *Nat. Rev. Mol. Cell Biol.* 15 (2014) 19–33.  
427 <https://doi.org/10.1038/nrm3721>.
- 428 [11] I.B. Halberg, K. Lyby, K. Wassermann, T. Heise, E. Zijlstra, L. Plum-Mörschel,  
429 Efficacy and safety of oral basal insulin versus subcutaneous insulin glargine in type 2  
430 diabetes: a randomised, double-blind, phase 2 trial, *Lancet Diabetes Endocrinol.* 7  
431 (2019) 179–188. [https://doi.org/10.1016/S2213-8587\(18\)30372-3](https://doi.org/10.1016/S2213-8587(18)30372-3).
- 432 [12] S.T. Buckley, T.A. Bækdal, A. Vegge, S.J. Maarbjerg, C. Pyke, J. Ahnfelt-Rønne,  
433 K.G. Madsen, S.G. Schéele, T. Alanentalo, R.K. Kirk, B.L. Pedersen, R.B.  
434 Skyggebjerg, A.J. Benie, H.M. Strauss, P.-O. Wahlund, S. Bjerregaard, E. Farkas, C.  
435 Fekete, F.L. Søndergaard, J. Borregaard, M.-L. Hartoft-Nielsen, L.B. Knudsen,  
436 Transcellular stomach absorption of a derivatized glucagon-like peptide-1 receptor  
437 agonist, *Sci. Transl. Med.* 10 (2018) eaar7047.  
438 <https://doi.org/10.1126/scitranslmed.aar7047>.
- 439 [13] A. Banerjee, J. Lee, S. Mitragotri, Intestinal mucoadhesive devices for oral delivery  
440 of insulin, *Bioeng. Transl. Med.* 1 (2016) 338–346. <https://doi.org/10.1002/btm2.10015>.
- 441 [14] K. Whitehead, Z. Shen, S. Mitragotri, Oral delivery of macromolecules using  
442 intestinal patches: applications for insulin delivery, *J. Control. Release.* 98 (2004) 37–  
443 45. <https://doi.org/10.1016/j.jconrel.2004.04.013>.
- 444 [15] A. Ahmed, C. Bonner, T.A. Desai, Bioadhesive microdevices with multiple  
445 reservoirs: a new platform for oral drug delivery, *J. Control. Release.* 81 (2002) 291–  
446 306. [https://doi.org/10.1016/S0168-3659\(02\)00074-3](https://doi.org/10.1016/S0168-3659(02)00074-3).
- 447 [16] J.R. Jørgensen, M.L. Jepsen, L.H. Nielsen, M. Dufva, H.M. Nielsen, T. Rades, A.  
448 Boisen, A. Müllertz, Microcontainers for oral insulin delivery – *In vitro* studies of  
449 permeation enhancement, *Eur. J. Pharm. Biopharm.* 143 (2019) 98–105.  
450 <https://doi.org/10.1016/j.ejpb.2019.08.011>.



- 451 [17] J.R. Jørgensen, F. Yu, R. Venkatasubramanian, L.H. Nielsen, H.M. Nielsen, A.  
452 Boisen, T. Rades, A. Müllertz, *In vitro*, *ex vivo* and *in vivo* evaluation of microcontainers  
453 for oral delivery of insulin, *Pharmaceutics*. 12 (2020) 48.  
454 <https://doi.org/10.3390/pharmaceutics12010048>.
- 455 [18] S. Saphier, A. Rosner, R. Brandeis, Y. Karton, Gastro intestinal tracking and gastric  
456 emptying of solid dosage forms in rats using X-ray imaging, *Int. J. Pharm.* 388 (2010)  
457 190–195. <https://doi.org/10.1016/j.ijpharm.2010.01.001>.
- 458 [19] A. Banerjee, K. Ibsen, T. Brown, R. Chen, C. Agatemor, S. Mitragotri, Ionic liquids  
459 for oral insulin delivery, *PNAS*. 115 (2018) 7296–7301.  
460 <https://doi.org/10.1073/pnas.1722338115>.
- 461 [20] S.K. Srivastava, F. Ajalloueiian, A. Boisen, Thread-Like Radical-Polymerization via  
462 Autonomously Propelled (TRAP) Bots, *Adv. Mater.* 31 (2019) 1901573.  
463 <https://doi.org/10.1002/adma.201901573>.
- 464 [21] L.H. Nielsen, S.S. Keller, A. Boisen, Microfabricated devices for oral drug delivery,  
465 *Lab. Chip*. 18 (2018) 2348–2358. <https://doi.org/10.1039/C8LC00408K>.
- 466 [22] K. Vdoviaková, E. Petrovová, M. Maloveská, L. Krešáková, J. Teleky, M.Z.J. Elias,  
467 D. Petrášová, Surgical anatomy of the gastrointestinal tract and its vasculature in the  
468 laboratory rat, *Gastroenterol. Res. Pract.* 2016 (2016) 2632368.  
469 <https://doi.org/10.1155/2016/2632368>.
- 470 [23] S. Harloff-Helleberg, L.H. Nielsen, H.M. Nielsen, Animal models for evaluation of  
471 oral delivery of biopharmaceuticals, *J. Control. Release*. 268 (2017) 57–71.  
472 <https://doi.org/10.1016/j.jconrel.2017.09.025>.
- 473 [24] A. Fjellestad-Paulsen, P. Höglund, S. Lundin, O. Paulsen, Pharmacokinetics of 1-  
474 deamino-8-d-arginine vasopressin after various routes of administration in healthy  
475 volunteers, *Clin. Endocrinol. (Oxf.)*. 38 (1993) 177–182. <https://doi.org/10.1111/j.1365-2265.1993.tb00990.x>.
- 476
- 477 [25] J. Wang, V. Yadav, A.L. Smart, S. Tajiri, A.W. Basit, Toward oral delivery of  
478 biopharmaceuticals: An assessment of the gastrointestinal stability of 17 peptide drugs,  
479 *Mol. Pharm.* 12 (2015) 966–973. <https://doi.org/10.1021/mp500809f>.
- 480 [26] V. Grabovac, F. Föger, A. Bernkop-Schnürch, Design and *in vivo* evaluation of a  
481 patch delivery system for insulin based on thiolated polymers, *Int. J. Pharm.* 348  
482 (2008) 169–174. <https://doi.org/10.1016/j.ijpharm.2007.06.052>.
- 483 [27] T. Flanagan, Potential for pharmaceutical excipients to impact absorption: A  
484 mechanistic review for BCS Class 1 and 3 drugs, *Eur. J. Pharm. Biopharm.* 141 (2019)  
485 130–138. <https://doi.org/10.1016/j.ejpb.2019.05.020>.
- 486 [28] L. Ceseracciu, J.A. Heredia-Guerrero, S. Dante, A. Athanassiou, I.S. Bayer, Robust  
487 and biodegradable elastomers based on corn starch and polydimethylsiloxane  
488 (PDMS), *ACS Appl. Mater. Interfaces*. 7 (2015) 3742–3753.  
489 <https://doi.org/10.1021/am508515z>.
- 490 [29] H. Daemi, S. Rajabi-Zeleti, H. Sardon, M. Barikani, A. Khademhosseini, H.  
491 Baharvand, A robust super-tough biodegradable elastomer engineered by

- 492 supramolecular ionic interactions, *Biomaterials*. 84 (2016) 54–63.  
493 <https://doi.org/10.1016/j.biomaterials.2016.01.025>.
- 494 [30] Y. Wang, G.A. Ameer, B.J. Sheppard, R. Langer, A tough biodegradable elastomer,  
495 *Nat. Biotechnol.* 20 (2002) 602–606. <https://doi.org/10.1038/nbt0602-602>.
- 496 [31] B.G. Amsden, Biodegradable elastomers in drug delivery, *Expert Opin. Drug Deliv.*  
497 5 (2008) 175–187. <https://doi.org/10.1517/17425247.5.2.175>.
- 498 [32] L.H. Nielsen, S.S. Keller, K.C. Gordon, A. Boisen, T. Rades, A. Müllertz, Spatial  
499 confinement can lead to increased stability of amorphous indomethacin, *Eur. J. Pharm.*  
500 *Biopharm.* 81 (2012) 418–425. <https://doi.org/10.1016/j.ejpb.2012.03.017>.  
501